

# Large Difference in the Elastic Properties of fcc and hcp Hard-Sphere Crystals

Sander Pronk and Daan Frenkel

*FOM Institute for Atomic and Molecular Physics, Kruislaan 407, 1098 SJ Amsterdam, The Netherlands*  
(Received 8 April 2003; published 23 June 2003)

We report a numerical calculation of the elastic constants of the fcc and hcp crystal phases of monodisperse hard-sphere colloids. Surprisingly, some of these elastic constants are very different (up to 20%), even though the free-energy, pressure, and bulk compressibility of the two crystal structures are very nearly equal. As a consequence, a moderate deformation of a hard-sphere crystal may make the hcp phase more stable than the fcc phase. This finding has implications for the design of patterned templates to grow colloidal hcp crystals. We also find that, below close-packing, there is a small, but significant, difference between the distances between hexagonal layers ( $c/a$  ratios) of fcc and hcp crystals.

DOI: 10.1103/PhysRevLett.90.255501

PACS numbers: 62.20.Dc, 82.70.Dd

The simplest regular close-packed structures of hard, spherical particles are the face-centered-cubic (fcc) and hexagonal-close-packed (hcp) structures (see Fig. 1). Close to melting, the Helmholtz free energies of these two crystal structures differ by less than 0.05% [1–3]. As a consequence, hard-sphere colloids (the experimental realization of elastic hard spheres) rarely crystallize directly into the more stable fcc structure. Rather, crystallization initially results in the formation of a randomly stacked crystal [4,5]. The latter then slowly transforms to the stable fcc structure [3,6–8]. However, pure hcp crystals have recently been grown by colloidal epitaxy on patterned templates [9]. At a given density, not only the free energies, but also the pressures and compressibilities of the fcc and hcp phases are very similar. One might therefore be tempted to suppose that these two crystal phases are similar in *all* their thermodynamic properties. Surprisingly, this is not the case. In this Letter, we present calculations of the elastic constants of fcc and hcp hard-sphere crystals. We show that some of these elastic constants may differ by as much as 20%. As a consequence, a moderate deformation of the hard-sphere crystal may change the relative stability of the two crystal phases.

A homogeneous deformation of a solid can be described by the transformation matrix  $\alpha_{ij}$  that relates the Cartesian coordinates  $x_j$  of a point in the undeformed solid, to the coordinates  $x'_i$  in the deformed solid:  $x'_i = \alpha_{ij}x_j$ , where summation of repeated indices is implied. The (isothermal) elastic constants of a crystal are most easily defined in terms of an expansion of the Helmholtz free energy  $F(N, V, T)$  in powers of the Lagrangian strains  $\eta_{ij}$  [10]:

$$F(\eta_{ij})/V = F(\mathbf{0})/V + T_{ij}(\mathbf{0})\eta_{ij} + \frac{1}{2}C_{ijkl}\eta_{ij}\eta_{kl} + \frac{1}{6}C_{ijklmn}\eta_{ij}\eta_{kl}\eta_{mn} + \dots \quad (1)$$

The Lagrangian strain parameters  $\eta_{ij}$  are related to the deformation matrix through  $\eta_{ij} \equiv \frac{1}{2}(\alpha_{ki}\alpha_{kj} - \delta_{ij})$ . In

Eq. (1), the coefficients  $T_{ij}(\mathbf{0})$  are simply the components of the stress tensor at zero deformation,  $C_{ijkl}$  are the second-order elastic constants,  $C_{ijklmn}$  are the third-order elastic constants, and so on. For a system under hydrostatic pressure  $P$ , the components of the stress tensor are  $T_{ij} = -\delta_{ij}P$ .

The fcc lattice has only three independent elastic constants [10] ( $C_{1111} \equiv C_{11}$ ,  $C_{1122} \equiv C_{12}$ , and  $C_{2323} \equiv C_{44}$  in the coordinate frame of the cubic unit cell). In what follows, we use this Voigt notation ( $C_{ij}$ ) to denote the second-order elastic constants.

In order to compare the elastic constants of the fcc and hcp crystals, we used the coordinate system shown in

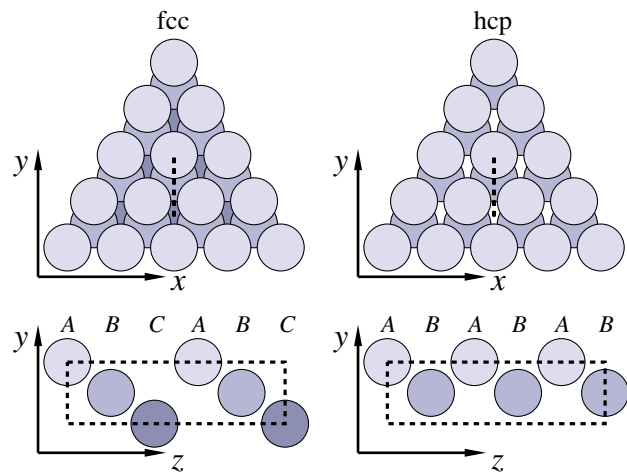


FIG. 1 (color online). Sketch of the structures of the regular close-packed fcc crystal (left) and hcp crystal (right). Inequivalent close-packed layers are labeled with the letters  $A$ ,  $B$ , and, in the case of fcc,  $C$ . An fcc crystal has  $ABCABC\dots$  stacking and an hcp crystal has  $ABABAB\dots$  stacking. The  $c/a$  ratio is the distance between two close-packed layers divided by the distance between neighboring particles in a close-packed layer. The figures show the definitions of the  $x$ ,  $y$ , and  $z$  directions referred to in the text.

Fig. 1, with the  $x$  and  $y$  directions in the hexagonal planes and the  $z$  direction perpendicular to these planes. For hcp (with hexagonal symmetry), there are six distinct elastic constants, five of which are independent [10]. To make a term-by-term comparison of the fcc and hcp elastic constant, it is convenient to ignore the full symmetry of the fcc crystal, and only use the fact that the crystal also has a lower rhombohedral symmetry. If the symmetry were really rhombohedral, the fcc crystal would have six independent elastic constants. But, if we take the full fcc symmetry into account, only three are linearly independent; the usual fcc elastic constants can be expressed as linear combinations of the rhombohedral elastic constants  $C'_{ij}$ :  $C_{11} = 4C'_{11} - 3C'_{33}$ ,  $C_{12} = C'_{33} + C'_{12} - C'_{11}$ , and  $C_{44} = C'_{33} - \frac{1}{2}(C'_{11} + C'_{12})$ .

We computed the elastic constants by calculating the stress response to a small applied strain, using molecular dynamics (MD) simulations [11]. At zero deformation, the stress response of a system with isotropic pressure  $P$  is given by a generalization of Hooke's law:

$$\frac{\partial^2 T_{ij}}{\partial \alpha_{rs} \partial \alpha_{tu}} = 2\delta_{tu}\delta_{rs}T_{ij} + (\delta_{it}\delta_{jr} + \delta_{ir}\delta_{jt})T_{su} - \delta_{ut}(\delta_{ir}T_{js} + \delta_{jr}T_{is}) - \delta_{sr}(\delta_{jt}T_{iu} + \delta_{it}T_{uj}) - \delta_{ut}C_{ijrs} + \delta_{it}C_{ujrs} + \delta_{jt}C_{iurs} - \delta_{sr}C_{ijtu} + \delta_{ir}C_{sjtu} + \delta_{jr}C_{istu} + \delta_{rt}C_{ijsu} + C_{ijrstu}. \quad (3)$$

The third-order elastic constants  $C_{ijrstu}$  appear in the last term.

The simulations were performed on systems with  $6 \times 6 \times 6 = 216$ ,  $12 \times 12 \times 12 = 1728$ , and  $24 \times 24 \times 24 = 13\,824$  particles. The maximum applied deformation at lower densities was  $4 \times 10^{-3}$ ; higher densities required even

TABLE I. Second-order elastic constants of fcc and hcp hard-sphere crystals at densities between the melting point and close packing. The values for the hcp structure with  $c/a = \sqrt{8/3}$  are shown in upright font. The (almost identical) results for a fully relaxed  $c/a$  ratio:  $c/a = \sqrt{8/3}(1 - 7.5 \times 10^{-4})$  at  $\phi = 0.543$ , are shown in italics. The simulation equilibration time was  $1 \times 10^4$  collisions per particle. Data were collected during typically  $2 \times 10^6$  collisions per particle for the 216 particle system, and  $6 \times 10^4$  collisions per particle for the 13 292 particle system. For each deformation, eight simulations were done at different strain amplitudes to check linearity of the stress response. The calculations of the stress-strain curve for each type of deformation involved simulations totaling  $6.4 \times 10^9$  collisions (one week on an Athlon 1600+ CPU).

$\phi$	$N$		$C'_{11}$	$C'_{12}$	$C'_{13}$	$C'_{14}$	$C'_{33}$	$C'_{44}$
0.543	13 292	fcc	90.51(6)	13.56(7)	7.51(7)	-8.77(4)	96.7(1)	32.22(6)
		hcp	87.39(8)	15.95(7)	7.7(1)	0	96.56(9)	33.79(4)
		<i>hcp</i>	<i>87.0(1)</i>	<i>15.82(9)</i>	<i>7.83(8)</i>	<i>0</i>	<i>97.1(1)</i>	<i>33.90(5)</i>
0.543	216	fcc	90.50(8)	13.8(1)	7.57(8)	-8.75(6)	97.0(1)	32.4(1)
		hcp	87.39(7)	16.6(1)	7.56(9)	0	96.67(9)	35.0(1)
0.550	216	fcc	99.41(9)	15.2(1)	8.4(1)	-9.65(4)	106.16(8)	35.76(4)
		hcp	95.88(6)	17.9(1)	8.6(1)	0	106.1(1)	37.38(7)
0.576	13 292	fcc	146.42(8)	21.86(7)	12.1(1)	-13.82(6)	156.1(1)	52.33(5)
		hcp	142.1(1)	25.64(7)	12.36(8)	0	155.78(9)	54.56(4)
0.576	216	fcc	146.1(1)	21.8(2)	12.1(1)	-14.3(1)	156.3(3)	52.8(4)
		hcp	141.8(1)	25.8(1)	12.44(9)	0	156.1(4)	54.9(1)
0.628	216	fcc	366.4(6)	51.6(4)	26.4(5)	-35.4(1)	392(1)	133.7(2)
		hcp	356.9(4)	60.3(6)	27.3(3)	0	390(1)	138.2(1)
0.681	216	fcc	1463(3)	189(2)	89(2)	-145(2)	1563(3)	535(2)
		hcp	1423(3)	223(3)	97(1)	0	1559(2)	557(2)
0.733	216	fcc	$1.10(1) \times 10^5$	$1.28(1) \times 10^4$	$6.1(2) \times 10^3$	$-1.05(3) \times 10^4$	$1.17(2) \times 10^5$	$4.05(4) \times 10^4$
		hcp	$1.08(1) \times 10^5$	$1.52(1) \times 10^4$	$5.4(1) \times 10^3$	0	$1.17(1) \times 10^5$	$4.08(1) \times 10^4$

smaller deformations to keep the stress response linear. The measured elastic constants between the melting point (packing fraction  $\phi = 0.543\,29$  [17]) and close packing are given in Table I.

At all densities, the values of the fcc and hcp elastic constants differ significantly (see Fig. 2). The relative differences between the elastic constants appear to remain approximately constant over the entire density range. The largest difference between fcc and hcp (up to 20%) was found for  $C'_{12}$ . Yet, the compressibilities of the two phases are identical to within the measurement error. For instance, at melting,  $K_{\text{fcc}}^T = 0.024\,22(5)$  vs  $K_{\text{hcp}}^T = 0.024\,24(5)$  (for 1728 particles). We computed these compressibilities in two ways: (a) from the appropriate linear combination of elastic constants and (b) directly from the equation of state [18]. The results are the same, to within the statistical error. At the same density, the pressures of the fcc and hcp phases are also very similar:  $P_{\text{fcc}} = 11.568(1)$  and  $P_{\text{hcp}} = 11.571(1)$ . Finally, the free energies differ only by about  $1.12(4) \times 10^{-3} k_B T$  per particle [1–3].

The difference between the fcc and hcp elastic constants is surprising because, already in 1967, Stillinger and Salsburg [19] had pointed out that a simple free-volume model predicts that the fcc and hcp elastic constants should be equal. However, they also showed that pair and triplet correlation effects can lead to differences. Still, we were surprised by the magnitude of the computed differences, in particular, for  $C'_{12}$ . To double check our calculations of the elastic constants, we performed a second, fully independent calculation where we directly computed the free energy of the crystals in various states of deformation. The free energy of the (deformed and undeformed) crystals was calculated using a 20-point

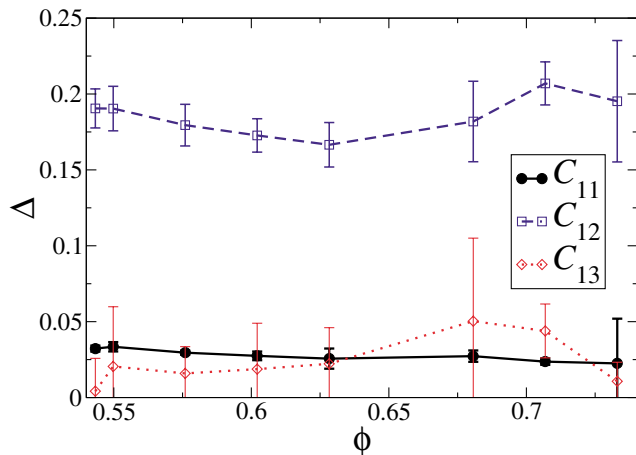


FIG. 2 (color online). Relative difference  $\Delta \equiv |C'_{ab}^{\text{fcc}} - C'_{ab}^{\text{hcp}}|/C'_{ab}^{\text{fcc}}$  between fcc and hcp  $C'_{11}$ ,  $C'_{12}$ , and  $C'_{13}$  elastic constants as a function of packing fraction  $\phi$ . The results shown were obtained in simulations of a system of 216 particles, with  $c/a = \sqrt{8/3}$ . The curves only serve as guides to the eye.

Einstein integration [17]. We found that the results obtained by the two methods were completely consistent. For example, in Fig. 3, we show the results of the two calculations for free-energy change due to a deformation of the form

$$\alpha_{ij} = \begin{pmatrix} 1 + \xi & 0 & 0 \\ 0 & 1/(1 + \xi) & 0 \\ 0 & 0 & 1 \end{pmatrix}. \quad (4)$$

To lowest order in  $\xi$ ,  $\Delta F/V = (-2T_{xx} + C_{11} - C_{12})\xi^2$ , for this deformation. As the figure shows, the differences in elastic constants  $C'_{11}$  and  $C'_{12}$ , for fcc and hcp, are so large that a deformation of 1.2% is enough to make hcp more stable than fcc. The free-energy increase of the fcc phase due to a deformation of 2% is  $\Delta f_{\text{fcc}} = 1.93(1) \times 10^{-2}$ , while for hcp it is only  $\Delta f_{\text{hcp}} = 1.66(1) \times 10^{-2}$ . Figure 3 also shows the effect of the third-order elastic constants. To within the statistical accuracy of our simulations, the relevant third-order elastic constants (see Table II), were found to be the same for fcc and hcp. Hence, they do not affect the free-energy difference between the two lattices.

For the undeformed fcc system, all three diagonal components of the pressure tensor are equal. However, this does not hold for a hcp system at the same  $c/a$  ratio (i.e., for the same spacing between the close-packed [111] planes). If we fix the  $c/a$  ratio at the fcc value ( $\sqrt{8/3}$ ), the stresses exhibit a slight anisotropy. For the 13 292 particle system  $T_{xx}$  and  $T_{yy}$  are equal (as they should be):  $T_{xx} = -11.587(1)$ ,  $T_{yy} = -11.588(1)$ . However,  $T_{zz}$  is significantly different:  $T_{zz} = -11.537(1)$ . From Eq. (1), we can derive what change in the  $c/a$  ratio is needed to make the pressure isotropic. We find that, at melting, isotropy is

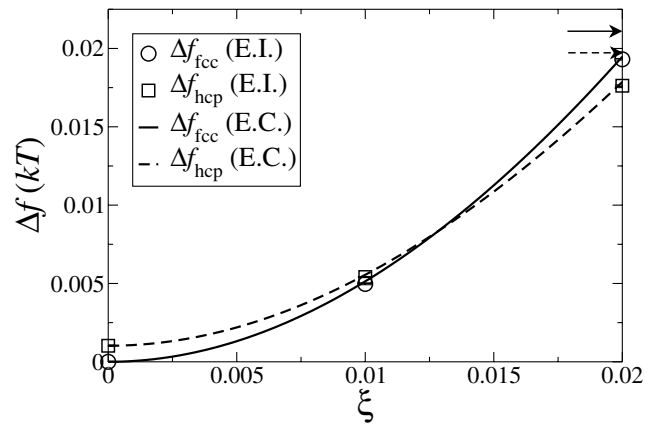


FIG. 3. Variation of the fcc and hcp free energy with deformation  $\xi$  [see Eq. (4)]. The symbols indicate the results of Einstein free-energy calculations (see text). The continuous curves were computed on the basis of the calculated second and third order elastic constants. The error bars of the Einstein free-energy calculations are about one-sixth the size of the symbols. The two horizontal arrows show the predictions for  $\Delta f$  obtained by neglecting the third-order elastic constants.

TABLE II. Values for the computed third-order elastic constants at melting ( $\phi = 0.54329$ ). These numbers were obtained for fcc and hcp systems containing 13 292 particles.

	fcc	hcp
$C'_{111}$	$-2.0(1) \times 10^3$	$-2.1(1) \times 10^3$
$C'_{112}$	$-7.3(9) \times 10^1$	$-7.9(9) \times 10^1$
$C'_{122}$	$-3.2(9) \times 10^2$	$-4.2(8) \times 10^2$
$C_{222}$	$-1.71(8) \times 10^3$	$-1.71(8) \times 10^3$

restored for a  $c/a$  ratio of  $\sqrt{8/3}[1 - 7.5(2) \times 10^{-4}]$ . At higher densities, this value approaches the close-packing value  $c/a = \sqrt{8/3}$ , as can be seen in Fig. 4. Stillinger and Salsburg [19] used the cell-cluster method to estimate the difference of the fcc and hcp  $c/a$  ratios. Our simulations show that, close to melting, the effect is 1 order of magnitude larger than predicted. The free-energy difference between the equilibrium hcp and fcc crystals is only slightly changed by this relaxation of the hcp  $c/a$  ratio: It becomes  $1.050(5) \times 10^{-3} k_B T$  per particle for  $N = 13\,292$  at melting.

As can be seen from the results in Table I for  $\phi = 0.543$ —where the  $c/a$  ratio differs most from fcc—the effect of relaxing  $c/a$  to its equilibrium value is barely significant. For this reason, most hcp elastic constants in Table I were computed for  $c/a = \sqrt{8/3}$ . The table also shows that the elastic constants depend somewhat on system size, but the effect is too small to change the qualitative picture.

In colloidal-epitaxy experiments [9], the best hcp crystals were obtained when the patterned template was stretched by 2.6% with respect to the expected lattice spacing at the experimental packing fraction ( $\phi = 0.68$ ). The templates used matched a diagonal cut through the  $xy$  plane of Fig. 1. Together with the stress produced by gravity (resulting in a strain perpendicular to the tem-

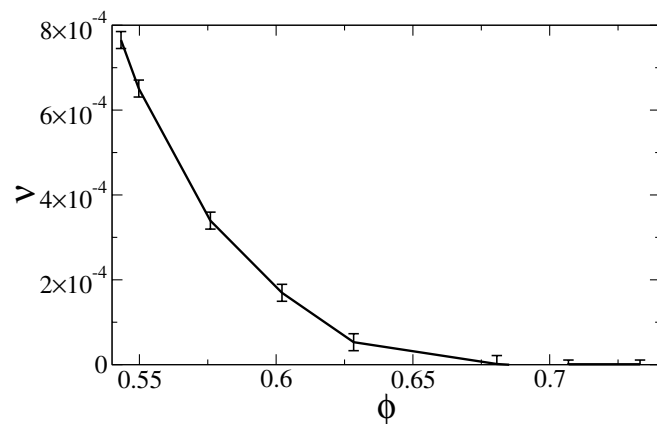


FIG. 4. Equilibrium anisotropy ( $\nu \equiv 1 - \frac{c}{a}/\sqrt{8/3}$ ) for the hcp hard sphere crystal as a function of packing fraction.

plate plane of  $-2.8\%$ ), this strain is comparable to the strain of Eq. (4) and would result in a free-energy difference of about  $3 \times 10^{-2} k_B T$  per particle *in favor* of hcp. The present simulation results may help experimentalists in designing optimal templates to grow selectively colloidal hcp or fcc crystals.

We thank Jacob Hoogenboom (Universiteit Twente) for inspiring discussions about his experimental work. The work of the FOM institute is part of the research program of the Foundation for Fundamental Research on Matter (FOM) and was made possible through financial support by the Dutch Foundation for Scientific Research (NWO).

- [1] P. Bolhuis, D. Frenkel, S.-C. Mau, and D. A. Huse, *Nature* (London) **388**, 235 (1997).
- [2] A. D. Bruce, N. B. Wilding, and G. J. Ackland, *Phys. Rev. Lett.* **79**, 3002 (1997).
- [3] S. Pronk and D. Frenkel, *J. Chem. Phys.* **110**, 4589 (1999).
- [4] J. Zhu, M. Li, R. Rogers, W. Meyer, R. H. Ottewill, STS-73 Space Shuttle Crew, W. B. Russel, and P. M. Chaikin, *Nature* (London) **387**, 883 (1997).
- [5] A. V. Petukhov, I. P. Dolbnya, D. G. A. L. Aarts, G. J. Vroege, and H. N. W. Lekkerkerker, *Phys. Rev. Lett.* **90**, 028304 (2003).
- [6] Z. Cheng, P. M. Chaikin, J. Zhu, W. B. Russel, and W. V. Meyer, *Phys. Rev. Lett.* **88**, 015501 (2002).
- [7] W. K. Kegel and J. K. G. Dhont, *J. Chem. Phys.* **112**, 3431 (2000).
- [8] V. C. Martellozzo, A. B. Schofield, W. C. K. Poon, and P. N. Pusey, *Phys. Rev. E* **66**, 021408 (2002).
- [9] J. P. Hoogenboom, A. K. van Langen-Suurling, J. Romijn, and A. van Blaaderen, *Phys. Rev. Lett.* **90**, 138301 (2003).
- [10] D. C. Wallace, in *Solid State Physics: Advances in Research and Applications*, edited by H. Ehrenreich, F. Seitz, and D. Turnbull (Academic, New York, 1970), pp. 301–404.
- [11] D. Frenkel and A. J. C. Ladd, *Phys. Rev. Lett.* **59**, 1169 (1987).
- [12] D. C. Rapaport, *J. Comput. Phys.* **34**, 184 (1980).
- [13] M. P. Allen and D. J. Tildesley, *Computer Simulation of Liquids* (Oxford University Press, Oxford, 1987).
- [14] M. Sprik, R. W. Impey, and M. L. Klein, *Phys. Rev. B* **29**, 4368 (1984).
- [15] K. V. Tretiakov and K. W. Wojciechowski, *J. Phys. Condens. Matter* **14**, 1261 (2002).
- [16] M. Parrinello and A. Rahman, *Phys. Rev. Lett.* **45**, 1196 (1980).
- [17] D. Frenkel and B. Smit, *Understanding Molecular Simulation* (Academic, London, 2002), 2nd ed.
- [18] R. J. Speedy, *J. Phys. Condens. Matter* **10**, 4387 (1998).
- [19] F. H. Stillinger and Z. W. Salsburg, *J. Chem. Phys.* **46**, 3962 (1967). As the cell-cluster expansion converges poorly, its numerical predictions differ very considerably (more than 100%) from the simulation data.